

UCSF

UC San Francisco Previously Published Works

Title

Trial Readiness of Cavernous Malformations With Symptomatic Hemorrhage, Part II: Biomarkers and Trial Modeling.

Permalink

<https://escholarship.org/uc/item/5h93b8h7>

Journal

Stroke, 55(1)

Authors

Hage, Stephanie
Kinkade, Serena
Girard, Romuald
[et al.](#)

Publication Date

2024

DOI

10.1161/STROKEAHA.123.044083

Peer reviewed



HHS Public Access

Author manuscript

Stroke. Author manuscript; available in PMC 2025 January 01.

Published in final edited form as:

Stroke. 2024 January ; 55(1): 31–39. doi:10.1161/STROKEAHA.123.044083.

Trial Readiness of Cavernous Malformations with Symptomatic Hemorrhage. Part II: Biomarkers and Trial Modeling

Stephanie Hage, MD,

Neurovascular Surgery Program, Department of Neurological Surgery, University of Chicago Medicine and Biological Sciences, Chicago, IL

Serena Kinkade, BS,

Neurovascular Surgery Program, Department of Neurological Surgery, University of Chicago Medicine and Biological Sciences, Chicago, IL

Romuald Girard, PhD,

Neurovascular Surgery Program, Department of Neurological Surgery, University of Chicago Medicine and Biological Sciences, Chicago, IL

Kelly D. Flemming, MD,

Department of Neurology, Mayo Clinic, Rochester, MN

Helen Kim, PhD,

Center for Cerebrovascular Research, Department of Anesthesiology and Perioperative Care, University of California San Francisco, San Francisco, CA

Michel T. Torbey, MD,

Department of Neurology, University of New Mexico, Albuquerque, NM

Judy Huang, MD,

Department of Neurosurgery, Johns Hopkins University Medical Institutions, Baltimore, MD

John Huston III, MD,

Department of Radiology, Mayo Clinic, Rochester, MN

Yunhong Shu, PhD,

Department of Radiology, Mayo Clinic, Rochester, MN

Reed G. Selwyn, PhD,

Blaine L. Hart, MD,

Correspondence to: Issam A. Awad, MD, Department of Neurological Surgery, University of Chicago Medicine, Department of Neurological Surgery, 5841 South Maryland Avenue, Room J341, Chicago, IL 60637, USA. iawad@uchicago.edu.

Disclosures

IAA is consultant and HK oversees Data and Safety Monitoring Board for Neurelis, Inc. IAA reports compensation from Medicoegal consulting for expert witness services. SK reports employment by UChicago. HK and KDF are consultants for Recursion Pharmaceuticals. JHuang is Director for American Board of Neurological Surgery; reports compensation by Longevity Neuro Solutions; employment by School of Medicine, Johns Hopkins University; and other intellectual property for Fundamentals of Operative Neurosurgery. JHutson is a stockholder in Navinetics and Resoundant; grants from Batterman Family Foundation; compensation from EISAI INC; and a provisional patent for Brain MR Elastography licensed to Mayo Clinic. JLupo has a grant from GE Healthcare. MM is employed by Mind Research Network and consultant for Smart Soft Healthcare. KL and DH report funding from National Institute of Neurological Disorders and Stroke. NM reports employment by Johns Hopkins University. JIK is employed by the NIH; this report does not represent the official view of the NIH or any part of the US Federal Government, and no official support or endorsement of this article by the NIH is intended or should be inferred.

Marc C. Mabray, MD,

Department of Radiology, University of New Mexico, Albuquerque, NM

James Feghali, MD,

Department of Neurosurgery, Johns Hopkins University Medical Institutions, Baltimore, MD

Haris I. Sair, MD,

The Russell H. Morgan Department of Radiology and Radiological Science, Johns Hopkins School of Medicine, Baltimore, MD

Jared Narvid, MD,

Department of Radiology and Biomedical Imaging, University of California San Francisco, San Francisco, CA

Janine M. Lupo, PhD,

Department of Radiology and Biomedical Imaging, University of California San Francisco, San Francisco, CA

Justine Lee, BSN,

Neurovascular Surgery Program, Department of Neurological Surgery, University of Chicago Medicine and Biological Sciences, Chicago, IL

Agnieszka Stadnik, MS,

Neurovascular Surgery Program, Department of Neurological Surgery, University of Chicago Medicine and Biological Sciences, Chicago, IL

Roberto J. Alcazar-Felix, MD,

Neurovascular Surgery Program, Department of Neurological Surgery, University of Chicago Medicine and Biological Sciences, Chicago, IL

Robert Shenkar, PhD,

Neurovascular Surgery Program, Department of Neurological Surgery, University of Chicago Medicine and Biological Sciences, Chicago, IL

Nicholas Hobson, MS,

Neurovascular Surgery Program, Department of Neurological Surgery, University of Chicago Medicine and Biological Sciences, Chicago, IL

Dorothy DeBiase, BS,

Neurovascular Surgery Program, Department of Neurological Surgery, University of Chicago Medicine and Biological Sciences, Chicago, IL

Karen Lane, CCRP,

Brain Injury Outcomes Unit, Department of Neurology, Johns Hopkins University Medical Institutions, Baltimore, MD

Nichole A. McBee, MPH,

Brain Injury Outcomes Unit, Department of Neurology, Johns Hopkins University Medical Institutions, Baltimore, MD

Kevin Treine, BS,

Brain Injury Outcomes Unit, Department of Neurology, Johns Hopkins University Medical Institutions, Baltimore, MD

Noeleen Ostapkovich, MS,

Brain Injury Outcomes Unit, Department of Neurology, Johns Hopkins University Medical Institutions, Baltimore, MD

Ying Wang, MS,

Brain Injury Outcomes Unit, Department of Neurology, Johns Hopkins University Medical Institutions, Baltimore, MD

Richard E. Thompson, PhD,

Brain Injury Outcomes Unit, Department of Neurology, Johns Hopkins University Medical Institutions, Baltimore, MD

James I. Koenig, PhD,

National Institute of Neurological Disorders and Stroke, Bethesda, MD

Timothy Carroll, PhD,

Department of Diagnostic Radiology, The University of Chicago Medicine and Biological Sciences, Chicago, IL

Daniel F. Hanley Jr., MD,

Brain Injury Outcomes Unit, Department of Neurology, Johns Hopkins University Medical Institutions, Baltimore, MD

Issam A. Awad, MD

Neurovascular Surgery Program, Department of Neurological Surgery, University of Chicago Medicine and Biological Sciences, Chicago, IL

Abstract

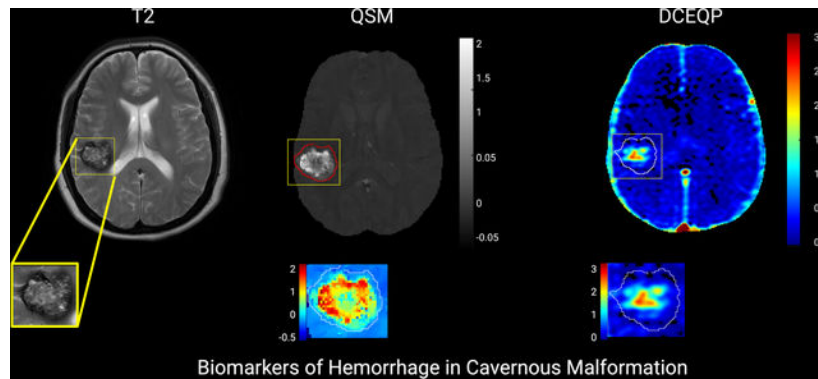
Background: Quantitative susceptibility mapping (QSM) and dynamic contrast enhanced quantitative perfusion (DCEQP) MRI sequences assessing iron deposition and vascular permeability were previously correlated with new hemorrhage in cerebral cavernous malformations (CM). We assessed their prospective changes in a multisite trial readiness project ([clinicaltrials.gov NCT03652181](https://clinicaltrials.gov/NCT03652181)).

Methods: Patients with CM and symptomatic hemorrhage (SH) in the prior year, without prior or planned lesion resection or irradiation were enrolled. Mean QSM and DCEQP of the SH lesion were acquired at baseline, and at 1- and 2-year follow-ups. Sensitivity and specificity of biomarker changes were analyzed in relation to predefined criteria for recurrent SH or asymptomatic change (AC). Sample size calculations for hypothesized therapeutic effects were conducted.

Results: We logged 143 QSM and 130 DCEQP paired annual assessments. Annual QSM change was greater in cases with SH than in cases without SH ($p=0.019$). Annual QSM increase by 6% occurred in 7 of 7 cases (100%) with recurrent SH and in 7 of 10 cases (70%) with AC during the same epoch, and 3.82 times more frequently than clinical events. DCEQP change had lower sensitivity for SH and AC than QSM change, and greater variance. A trial with smallest sample size would detect a 30% difference in QSM annual change during two years of follow-up in 34 or 42 subjects (one and two-tailed, respectively), power 0.8, alpha 0.05.

Conclusions: Assessment of QSM change is feasible and sensitive to recurrent bleeding in CM. Evaluation of an intervention on QSM percent change may be used as a time-averaged difference between 2 arms using a repeated measures analysis. DCEQP change is associated with lesser sensitivity and higher variability than QSM. These results are the basis of an application for certification by the U.S. F.D.A. of QSM as a biomarker of drug effect on bleeding in CM.

Graphical Abstract:



Keywords

cavernous angioma; cerebral cavernous malformation; biomarkers; quantitative susceptibility mapping; permeability; clinical trial

Introduction

Cerebral cavernous malformation (CM), also known as cavernous angioma is a common hemorrhagic vascular anomaly of the human brain, affecting > 1 million Americans. Although the risk of first symptomatic hemorrhage (SH) from a CM is very low (<1% per year), cases with SH carry a ten-fold risk of rebleeding with serious clinical sequelae¹. Asymptomatic bleeds in lesions can also herald future clinically relevant hemorrhage². Several drugs have been shown in pre-clinical studies to decrease CM bleeding, and are poised for clinical testing^{3–8}. Currently, clinical magnetic resonance imaging (MR) can detect a new bleed in CM, if performed within 4–6 weeks of hemorrhage but does not quantify the extent of bleeding. Awaiting new symptoms and performing MRI to detect a new bleed, can miss sub-clinical bleeds and the cumulative impact of repeated hemorrhages during follow-up. Clinical trials aimed at decreasing rates of recurrent symptoms cannot be realistically performed, with fewer than 200,000 CM cases with SH in the U.S. per year (meeting rare disease criteria), and rates of SH requiring potentially thousands of patients to confirm a drug effect.

Quantitative susceptibility mapping (QSM) is a noninvasive MRI technique that assesses iron content by quantifying the magnetic susceptibility of local tissues⁹. Iron content in surgically excised CM lesions precisely reflects the iron concentration in the same specimens assessed by mass spectrometry, and phantom studies have validated QSM assessment of ferric, ferrous and ferromagnetic iron concentrations¹⁰. Further, multisite validation of QSM acquisitions has been conducted using multiple instruments at different

institutions, confirming accuracy, precision and reproducibility¹¹. Researchers in Chicago and New Mexico optimized a second technique, dynamic contrast enhanced quantitative perfusion (DCEQP) on MRI in human subjects, reflecting mechanistically postulated vascular hyper-permeability in CMs^{12,13}.

Both QSM and DCEQP showed strong inter-observer agreement in QSM and DCEQP measurements, stability of both measurements in clinically stable CM lesions^{10,14,15}. As predicted by the conservation of mass hypothesis, CM lesions with greater permeability had higher lesional iron content (QSM)¹⁶, and lesional iron content was greater in older patients and in CMs with prior SH¹⁵. More recent studies demonstrated a significant increase of mean lesional QSM and DCEQP in lesions that had been stable clinically and on imaging for more than a year, and then manifested interval SH or growth during longitudinal follow-up, while these did not change in stable lesions¹⁴. There were tight, sensitive and specific thresholds of QSM and DCEQP increases in association with clinical events. Therefore, it is postulated that the QSM and DCEQP may be used as *in vivo* measures of hemorrhagic activity and vascular leak, respectively, and may reflect sensitive, clinically meaningful therapeutic effect in human CAs.

To date, only a small pilot study at a single site has assessed lesional QSM change during prospective follow-up of CM patients who had suffered a SH within the prior year¹⁷. The Trial Readiness project ([clinicaltrials.gov NCT03652181](https://clinicaltrials.gov/NCT03652181)) aimed to characterize CM cases with SH at multiple sites, who might participate in therapeutic clinical trials. In an accompanying paper¹⁸, we report prospective rates of clinical rebleeding and changes in functional status and quality of life assessments. Here, we here present changes in lesional iron content and vascular permeability, assessed by QSM and DCEQP respectively, during longitudinal follow-up.

Patients and Methods

Study Design, Subject Enrollment and Cases Contributing Paired Biomarker Data

The study protocol and baseline features of trial eligible CM subjects with SH were published previously^{19,20}. Details of study design and inclusion exclusion criteria are presented in the Supplemental Methods. We followed herein the guidelines for Strengthening the Reporting of Observational Studies in Epidemiology (STROBE) (<https://www.strobe-statement.org/>). The study Protocol was approved by the Central Institutional Review Board at the University of Chicago Medicine and written informed consent was obtained from patients.

Subjects were enrolled at U.S. high volume centers and followed for up to 2 years. Clinical and research MRI studies were also conducted at enrollment and at the end of each year of follow-up. An epoch of follow-up was defined as 1 year \pm 1 month, with the 1st epoch being from enrollment (baseline) to the year 1 follow-up, and the 2nd epoch from year 1 to year 2 follow-ups. At each visit (baseline, year 1 and year 2), the patient was queried about new or worsening symptoms and the MRI was assessed for any lesional changes. Lesions were labeled as having a detected SH or asymptomatic change (AC) during the 1st or/and 2nd epoch. An SH was defined by new lesional hemorrhage documented by

imaging and attributable by the CM clinician to new or worsening symptoms. An AC was defined as lesional growth of ≥ 3 mm or new bleeding on comparable T2 or T1-weighted images respectively^{2,19} but without attributable new or worsening symptoms. The clinical and research MRI sequences^{11,19} were obtained in the same session. Any outside imaging obtained for any reason was reviewed, to ascertain any lesional SH or AC during the year.

By November 1, 2022, 121 subjects were due to their Year 1 follow-up, and 102 completed it, including 95 who also underwent the research MRI studies at their visit (93.1 % of subjects contributed paired research imaging biomarker data in the 1st epoch). Eighty subjects were due for their year 2 follow-up, of whom 69 completed clinical follow-up and 59 completed the year 2 research MRI sequences (84.3% of subjects contributed paired research biomarker data in the 2st epoch). In total, 277 QSM and 276 DCEQP sequences were acquired.

Biomarker Data Acquisition and Post-processing

DCEQP and QSM scans across all five sites utilized a 3-Tesla field strength scanner with an eight-channel head coil for acquisition. The quantitative measurement of MRI biomarkers has been previously validated across instrument platforms and institutions using both static and dynamic phantom models¹¹. Detailed protocols of research imaging have been previously published^{11,14,19,21} and are summarized in the Supplemental Methods. Figure 1 illustrates conventional MRI, QSM and DCEQP assessments of the SH lesion. We excluded research sequences which were corrupted during acquisition, included artifacts, or did not cover the SH lesion, and hence did not contribute usable QSM or DCEQP values.

Definition of Biomarker Outcomes

Annual change in mean QSM and DCEQP of the SH lesion were proposed as monitoring biomarkers of respective change in lesional iron content and permeability, to be targeted for potential treatment effect in clinical trials^{17,19,22}.

Previous studies had established biologic plausibility and receiver operation curves (ROC) analyses of the QSM and DCEQP mean yearly change in initially stable CM (without a SH event in the prior year), had identified an increase in mean lesional QSM of $\geq 5.81\%$ (sensitivity 82.3%; specificity 88.89%) and an increase of $\geq 39.59\%$ (sensitivity 78.72%; specificity 88.89%) in mean lesional DCEQP were associated with new SH during annual follow-up¹⁴. We thus defined and prespecified two categorical threshold “biomarker events” as $\geq 6\%$ yearly change in mean lesional QSM and $\geq 40\%$ annual change in mean lesional DCEQP.

Statistical Methods

All analyses were performed using STATA 17.0 (Stata Corp, College Station, Texas).

Changes in mean lesional QSM or DCEQP were calculated as relative percent changes for each annual epoch:

$$\text{Relative \% change of QSM or DCEQP} = \frac{(QSM \text{ or DCEQP}_{t1} - QSM \text{ or DCEQP}_{t0})}{QSM \text{ or DCEQP}_{t0}} \times 100$$

t0: 1ST point in the epoch t1: 2nd point in the epoch

Analyses were applied on annual % change in lesional QSM or DCEQP as continuous variables. Wilcoxon signed rank test compared the distributions of % change in lesional QSM or DCEQP during the 1st and the 2nd annual epochs. Mann Whitney U test compared the distributions of % change in lesional QSM or DCEQP in epoch-years with no clinical events and those with a clinical event (SH or asymptomatic change [AC]) documented during the epoch-year. No patient contributed more than one paired QSM or DCEQP during a single epoch-year.

Statistical analyses on potential confounders and effects of lesion size and location are presented in legends of the respective Supplemental Tables.

Trial Simulation and Sample Size Calculations

Based on variance and correlation of % biomarker changes in 1st and 2nd epochs, sample size calculations were conducted to power trials for a hypothesized therapeutic effect on mean lesional QSM change or mean lesional DCEQP change. The effect sizes modeled were based on the minimum clinically significant changes between groups (relative risk reduction of 20%, 25% and 30%), as documented in preclinical studies^{4,5,22}. We used the variances of the mean percent change for QSM or DCEQP for each epoch as well as the correlation of the change in Epoch 1 and 2 observed in our study to estimate the SD of the mean change in each measure over both epochs. In estimating the sample sizes based on the two sample t-test that compared differences by treatment arm in the mean change for each measure over both epochs, we assumed power of 0.8 and alpha of 0.05 (two-tailed or one-tailed), 1:1 randomization, and patient follow-up for two years (2 paired biomarker assessments). The power of future trials based on hypothesized intervention effect on the annual rate of SH or the rate of a composite outcome (SH, AC or QSM threshold biomarker event) used the two-sample test of proportions, and also assumed a power of 0.8 and two-tailed and one-tailed alpha of 0.05. Necessary information to replicate the sample size estimates is provided in the respective Supplemental Tables summarizing the simulation results.

Results

Figure 2 shows the respective cohorts contributing to clinical and biomarker assessments, and SH and AC events in these cohorts. Respective contributions of research imaging at the multiple sites, and a comparison of cases with and without biomarker assessments are summarized in the Supplemental Tables 1–3.

Change in Mean Lesional QSM During Annual Follow-up of SH Lesions

Raw data on mean lesional QSM assessments are presented in the Supplemental Figure 1. Of 295 potential QSM sequences due by the 1st of November 2022 (123 at baseline, 102 at year 1, and 70 at year 2), 277 were conducted, hence 93.9% feasibility of QSM acquisition.

Of 277 acquired sequences, 269 were usable (97.1%) and contributed to 143 total pairs of QSM (91 and 52 QSM pairs in the 1st and 2nd annual epochs of follow-up, respectively). There were 3 cases with SH and 8 with AC during the 1st year, and 4 SH and 2 AC during the 2nd year, among cases with corresponding paired QSM assessments (Figure 1). The overall mean QSM yearly-change was +17.52 (SD 73.27). QSM yearly-change during epoch 1 (mean +16.33; SD 74.93) was significantly lower than in epoch 2 (mean +19.61; SD 70.96) (p 0.033) with a correlation of ρ -0.39 (Figure 3). There were no significant differences in QSM yearly-change between cases with SH (mean +34.64; SD 27.17) and cases with AC (mean +38.53; SD 59.36). QSM changes in cases with SH, and those with SH or AC were significantly higher than QSM change in cases with no clinical events (p 0.019 and 0.0043 respectively) (Figure 4). Except for greater mean lesional QSM at baseline and the end of the 2nd year in lesions >20 mm in maximum diameter than those < 10 mm, there was no significant effect of lesion size or location on mean lesional QSM or DCEQP values or their changes (Supplemental Tables 4–5).

A QSM increase by 6% was found in all 7 SH cases contributing paired QSM assessments, indicating 100% sensitivity for recurrent SH. A QSM increase by 6% occurred in 7 of 10 AC cases, with a sensitivity of 70% to ACs identified in the study. The 3 cases categorized as AC per prespecified criteria (increase of T1 signal or hemorrhagic lesion growth by > 3 mm) without QSM increase by 6% may have represented evolution of prior bleed rather than new bleeding, hence an imprecision of the definition of AC by predefined MRI criteria (Supplemental Figure 2). A QSM increase by 6% was documented in 51 pairs without SH or AC, a relative frequency 3.82 greater than the occurrence of clinical events.

Change in Mean Lesional DCEQP During Annual Follow-up of SH Lesions

Raw data on mean lesional DCEQP assessments are presented in the Supplemental Figure 1. Of 295 potential DCEQP sequences, 276 were acquired, hence a feasibility rate of 93.6%. Of these, 249 sequences were usable after processing, with a usability rate of 90.2%, contributing 130 DCEQP annual paired assessments. Three SH and 7 AC occurred during the 1st epoch, and 5 SH and 2 AC during the 2nd epoch among cases with corresponding paired DCEQP assessments (Figure 1). Mean lesional DCEQP yearly-change was +58.09 (SD +232.6). DCEQP yearly-change during the 1st epoch (mean +61.62; SD +248.8) was not significantly different from the change during the 2nd epoch (mean +52.45; SD +206.4) with a correlation of ρ -0.15 (Figure 5). DCEQP pairs with SH events had a higher mean lesional change (mean +179.9; SD +237.4) than DCEQP pairs without detected clinical events (mean +49.92; SD +235.5) (p 0.030). There was no significant difference in yearly DCEQP change in cases with AC events (mean +52.45; SD +175.8) and SH events (Figure 6). DCEQP annual increase was found in 6 of the 8 cases with recurrent SH cases indicating 75% sensitivity, and in 3 out of 9 AC cases with a sensitivity of 33.33%. The DCEQP increase 40% was identified in 43 pairs without SH or AC, 3 times more frequently than clinical events.

Trial Modeling

Sample sizes for potential trials were based on variance and co-correlation of % biomarker changes in 1st and 2nd epochs, a hypothesized therapeutic effect on mean lesional QSM or DCEQP change, a time-averaged difference between the two groups using a repeated measures analysis conducted as an unadjusted linear mixed model^{17,19,22}, assumed power of 0.8 and alpha of 0.05 (two-tailed or one-tailed), 1:1 randomization, and patient follow-up for two years (2 paired biomarker assessments). For an interventional effect of 30% reduction in QSM change, 42 (two-tailed) or 34 (one-tailed) subjects are sufficient, respectively (Supplemental Table 6) with two years follow-ups and two paired biomarker assessments per subject. Detecting a 20% reduction in QSM change would require 92 subjects if two-tailed test, and 72 subjects if one-tailed test. Because the variances and consequently the standard deviations of DCEQP yearly-change in both epochs were considerably higher, a clinical trial using DCEQP as a surrogate outcome would require hundreds to thousands of subjects in order to demonstrate a therapeutic effect (Supplemental Table 6).

We also considered the therapeutic effect on the frequency of SH, and of a composite categorical outcome of any SH, AC, or QSM biomarker increase $\geq 6\%$ per patient year of follow-up. This effectively counts cases with SH or AC (who did not undergo biomarker assessments in the epoch where they suffered the SH or AC), as well as those whose lesion showed a QSM increase $\geq 6\%$, (shown to be sensitive to lesional bleeding and more frequent than SH and AC events). There were overall 21 cases with SH in the trial readiness follow-up and biomarker validation cohort¹⁸, and 86 with SH, AC or QSM $\geq 6\%$ during 175 patients-years of follow-up. As the annual SH rate in this multisite clinical trial was 12.0%, this composite outcome rate was much more frequent at 49.2%. Trial sample sizes based on a change of SH rate alone versus composite outcome rate (SH, AC or QSM $\geq 6\%$) are presented in the Supplemental Table 7. To demonstrate a 30% reduction in SH rates, total sample sizes of 2218 (two-tailed) or 1746 (one-tailed) patient-years of follow-up are required, assuming a power of 0.8 and alpha of 0.05 (two-tailed or one-tailed), and 1:1 randomization. A 30% reduction of the composite outcome rate can be detected with 356 (two-tailed) or 274 (one-tailed) patient-years, or 178 and 137 patients followed for two years, assuming the same event rates in both years.

Discussion

We here demonstrate the feasibility and usability of QSM and DCEQP acquisitions during prospective follow-up of trial eligible CM subjects with recent SH. Among patients who came to the research sites for scheduled visits, 93.9% and 93.6% completed QSM and DCEQP acquisitions, respectively. Of these, 97.1% and 90.2% were usable. This likely reflected protocolized site initiation and education, phantom assessment of QSM and dynamic T1-weighted signal at each MRI instrument, the chaperoning of research imaging acquisition, including repeat acquisitions in cases of head movement or other technical problems¹¹. All imaging research sequences were post-processed at the Chicago imaging core. These results are very encouraging regarding potential imaging biomarker implementation in clinical trials, provided similar rigorous protocols are followed.

Published correlations of QSM and DCEQP changes in CMs had mostly addressed previously stable lesions¹⁴. Changes in lesions with recent SH would be expected to be more complex, as they include recovery from hemorrhage and greater likelihood of rebleeding. To date, only a small pilot study had assessed lesional QSM change during prospective follow-up of patients who had suffered a SH within the prior year¹⁷. During 22 patient-years of follow-up in 16 subjects, there were twice as many cases with a documented threshold biomarker event ($\geq 6\%$ QSM increase) as clinical events, and no clinical event occurred without such threshold increase in QSM. We here confirmed greater increases in QSM and DCEQP changes in lesions with a repeat SH or AC during the annual follow-up than in those without clinical events. We also confirmed an annual QSM change $\geq 6\%$, which had been associated with new SH in previously stable CMs, in every case with new SH during the same year (100% sensitivity). Sensitivity was lower for AC in lesions, although this partly suggests imprecise definition of new bleeding versus evolution of prior bleeding based on conventional MRI features.

An effect of atorvastatin versus placebo on percent change in mean lesional QSM in SH lesions has been postulated as a primary outcome of the ongoing prospective double-blind Phase I/IIA proof of concept trial ([clinicaltrials.gov: NCT02603328](https://clinicaltrials.gov/ct2/show/study/NCT02603328)), where patient enrollment has been completed and follow-up is underway of enrolled cases for two years²². A prior pilot study with a small number of cases addressed the effect of simvastatin on DCEQP in CM lesions²³. However, that study was underpowered and did not address lesions with recent SH specifically, nor did it use equivalent drug doses required for effect in preclinical studies^{5,6}.

Based on results herein at multiple sites, trial simulations endorse a very efficient sample size by using mean lesional annual percent QSM change as an outcome, and a time-averaged difference between the two groups using a repeated measures analysis, conducted as an unadjusted linear mixed model^{17,19,22}. With this approach, the most efficient trial model would detect a 30% relative risk reduction in QSM annual change with only 34 or 42 subjects (one and two-tailed, respectively), followed for two years, 1–1 assignment, power=0.8, and alpha=0.05. This is clinically meaningful and in line with effect sizes on iron deposition in preclinical models^{4–8}. Such efficient sample sizes are attractive for platform trials, and for assessing the comparative effects of multiple drugs or doses in a rare disease. Two-tailed trials would be needed for potential drugs where there may be concern about increasing or decreasing lesional bleeding (i.e., statins, aspirin), while one-tailed trials are applicable for drugs where there is no concern about increasing hemorrhage (i.e. propranolol). The results herein motivated an application under review by the United States Food and Drug Administration, Center for Drug Evaluation and Research Biomarker Qualification Program Drug Development Tool (DDT-BMQ-000127) to assess drug effects on lesional bleeding in CMs.

Lower feasibility, usability and sensitivity for SH, very high variances, and the need for repeated gadolinium administration, dampen enthusiasm for using DCEQP as a similar biomarker. In fact, sample size calculations endorsed the need for huge sample sizes, in comparison to QSM when targeting an effect on DCEQP change.

Since these simulations are derived from cases with paired QSM or DCEQP assessments, there is concern that they would not reflect cases with missing paired biomarker assessment, particularly cases with known SH or AC who underwent surgery or otherwise did not complete post-bleed biomarker assessments. Indeed, cases with SH were less likely to contribute paired biomarker assessments (Supplemental Table 1), possibly due to undergoing surgery after a documented SH. Also, males were less likely to contribute paired QSM assessments. One possible approach to adjust for missing biomarker data would be to impute the mean QSM change of cases with no clinical events in cases missing biomarker data and who had no SH/AC events, and the mean QSM change of SH or AC in cases missing biomarker data who had SH or AC events. Another option is to consider a composite outcome of any SH or AC or QSM biomarker increase $\geq 6\%$. This would effectively count cases with SH or AC who did not undergo biomarker assessments in the epoch where they suffered the SH or AC, as well as those whose lesion showed a QSM increase $\geq 6\%$, shown to be sensitive to lesional bleeding and biologically plausible. SH annual rate in this multisite clinical trial was 12.0% and this composite annual outcome rate was much more efficient 49.2%. A 30% relative risk reduction in two groups on the composite annual outcome rate can be detected with 356 (two-tailed) or 274 (one-tailed) patient-years, more efficient than with SH alone, but clearly less efficient than modeling on % lesional QSM change.

We only assessed changes in QSM and DCEQP during annual epochs of follow-up, and we cannot comment about the value of more frequent assessments. It is also unclear what is the timeline of increase of lesional QSM or DCEQP after a bleed, or its recovery. Among cases who completed paired biomarker assessments, SHs tended to cluster toward the end of the epoch (Supplemental Figure 3). This could be explained by greater likelihood of cases with recurrent SH undergoing surgery earlier in the epoch, and not completing paired biomarker assessments (Supplemental Table 1). Despite this clustering, there was a trend toward greater percent mean lesional QSM and DCEQP change when the SH occurred closer to the second biomarker acquisition, consistent with greater sensitivity to more recent bleeding.

We prespecified a percent change in annual mean lesional biomarker measures, based on pilot studies where absolute changes, median, maximum or minimum values were not as sensitive or specific in relation to clinical bleeding^{14,15}. The lesional border was defined on T2-weighted sequences for the assessments of the CM region of interest. We noted that maximal QSM areas often involved the CM periphery while DCEQP maximal values often involved the core of the lesion (Figure 1), although there were substantial heterogeneities (Supplemental Figure 2). More recently, Incerti, et al. reported maximal lesional QSM as a prognostic biomarker of bleeding in CMs,²⁴ but they did not specify how many pixels were considered for such maximal values, nor did they analyze mean lesional QSM or report changes in QSM over time. Sone, et al. from our team analyzed multiple derivations of permeability and perfusion (mean, median, upper or lower terciles, coefficient of variation, skewness, kurtosis, entropy, high-value cluster mean and area, as well as low-value cluster mean and area) from DCEQP acquisitions at a single point in time, as diagnostic and prognostic biomarkers of SH^{25,26}. In ongoing studies outside the scope of this report, we propose to analyze changes of these biomarker derivations over time in the Trial Readiness

cohort, explore artificial intelligence analysis of other features of QSM and DCEQP maps, and correlate QSM and DCEQP changes with plasma biomarkers of SH.

Supplementary Material

Refer to Web version on PubMed Central for supplementary material.

Source of Funding

Funded by the National Institute of Neurological Disorders and Stroke, National Institutes of Health (NIH) U01NS104157

Non-standard Abbreviations and Acronyms

AC	asymptomatic change
CM	cavernous malformation
DCEQP	dynamic contrast enhanced quantitative perfusion
MRI	magnetic resonance imaging
QSM	quantitative susceptibility mapping
SH	symptomatic hemorrhage
SD	standard deviation

References

1. Horne MA, Flemming KD, Su IC, Stapf C, Jeon JP, Li D, Maxwell SS, White P, Christianson TJ, Agid R, et al. Clinical course of untreated cerebral cavernous malformations: a meta-analysis of individual patient data. *Lancet Neurol.* 2016;15:166–173. [PubMed: 26654287]
2. Carrión-Penagos J, Zeineddine HA, Polster SP, Girard R, Lyne SB, Koskimäki J, Romanos S, Srinath A, Zhang D, Cao Y, et al. Subclinical imaging changes in cerebral cavernous angiomas during prospective surveillance. *J Neurosurg.* 2020;134:1147–1154. [PubMed: 32244216]
3. Snellings DA, Hong CC, Ren AA, Lopez-Ramirez MA, Girard R, Srinath A, Marchuk DA, Ginsberg MH, Awad IA, Kahn ML. Cerebral Cavernous Malformation: From Mechanism to Therapy. *Circ Res.* 2021;129:195–215. [PubMed: 34166073]
4. McKerracher L, Shenkar R, Abbinanti M, Cao Y, Peiper A, Liao JK, Lightle R, Moore T, Hobson N, Gallione C, et al. A Brain-Targeted Orally Available ROCK2 Inhibitor Benefits Mild and Aggressive Cavernous Angioma Disease. *Transl Stroke Res.* 2020;11:365–376. [PubMed: 31446620]
5. Shenkar R, Peiper A, Pardo H, Moore T, Lightle R, Girard R, Hobson N, Polster SP, Koskimäki J, Zhang D, et al. Rho Kinase Inhibition Blunts Lesion Development and Hemorrhage in Murine Models of Aggressive Pcd10/Ccm3 Disease. *Stroke.* 2019;50:738–744. [PubMed: 30744543]
6. Shenkar R, Shi C, Austin C, Moore T, Lightle R, Cao Y, Zhang L, Wu M, Zeineddine HA, Girard R, et al. RhoA Kinase Inhibition With Fasudil Versus Simvastatin in Murine Models of Cerebral Cavernous Malformations. *Stroke.* 2017;48:187–194. [PubMed: 27879448]
7. Shi C, Shenkar R, Zeineddine HA, Girard R, Fam MD, Austin C, Moore T, Lightle R, Zhang L, Wu M, et al. B-Cell Depletion Reduces the Maturation of Cerebral Cavernous Malformations in Murine Models. *J Neuroimmune Pharmacol.* 2016;11:369–377. [PubMed: 27086141]

8. Li W, Shenkar R, Detter MR, Moore T, Benavides C, Lightle R, Girard R, Hobson N, Cao Y, Li Y, et al. Propranolol inhibits cavernous vascular malformations by β 1 adrenergic receptor antagonism in animal models. *J Clin Invest*. 2021;131:e15490.
9. Eskreis-Winkler S, Zhang Y, Zhang J, Liu Z, Dimov A, Gupta A, Wang Y. The clinical utility of QSM: disease diagnosis, medical management, and surgical planning. *NMR Biomed*. 2017;30:e3668.
10. Tan H, Liu T, Wu Y, Thacker J, Shenkar R, Mikati AG, Shi C, Dykstra C, Wang Y, Prasad PV, et al. Evaluation of iron content in human cerebral cavernous malformation using quantitative susceptibility mapping. *Invest Radiol*. 2014;49:498–504. [PubMed: 24619210]
11. Hobson N, Polster SP, Cao Y, Flemming K, Shu Y, Huston J, Gerrard CY, Selwyn R, Mabray M, Zafar A, et al. Phantom validation of quantitative susceptibility and dynamic contrast-enhanced permeability MR sequences across instruments and sites. *J Magn Reson Imaging*. 2020;51:1192–1199. [PubMed: 31515878]
12. Hart BL, Taheri S, Rosenberg GA, Morrison LA. Dynamic contrast-enhanced MRI evaluation of cerebral cavernous malformations. *Transl Stroke Res*. 2013;4:500–506. [PubMed: 24323376]
13. Mikati AG, Khanna O, Zhang L, Girard R, Shenkar R, Guo X, Shah A, Larsson HB, Tan H, Li L, et al. Vascular permeability in cerebral cavernous malformations. *J Cereb Blood Flow Metab*. 2015;35:1632–1639. [PubMed: 25966944]
14. Girard R, Fam MD, Zeineddine HA, Tan H, Mikati AG, Shi C, Jesselson M, Shenkar R, Wu M, Cao Y, et al. Vascular permeability and iron deposition biomarkers in longitudinal follow-up of cerebral cavernous malformations. *J Neurosurg*. 2017;127:102–110. [PubMed: 27494817]
15. Tan H, Zhang L, Mikati AG, Girard R, Khanna O, Fam MD, Liu T, Wang Y, Edelman RR, Christoforidis G, et al. Quantitative Susceptibility Mapping in Cerebral Cavernous Malformations: Clinical Correlations. *AJNR Am J Neuroradiol*. 2016;37:1209–1215. [PubMed: 26965464]
16. Mikati AG, Tan H, Shenkar R, Li L, Zhang L, Guo X, Larsson HB, Shi C, Liu T, Wang Y, et al. Dynamic permeability and quantitative susceptibility: related imaging biomarkers in cerebral cavernous malformations. *Stroke*. 2014;45:598–601. [PubMed: 24302484]
17. Zeineddine HA, Girard R, Cao Y, Hobson N, Fam MD, Stadnik A, Tan H, Shen J, Chaudagar K, Shenkar R, et al. Quantitative susceptibility mapping as a monitoring biomarker in cerebral cavernous malformations with recent hemorrhage. *J Magn Reson Imaging*. 2018;47:1133–1138. [PubMed: 28791783]
18. Flemming KD, Kim H, Hage S, Mandrekar J, Girard R, Torbey M, Huang J, Huston J, Shu Y, Lanzino G, et al. Prospective Follow up of Cavernous Angiomas with Symptomatic Hemorrhage (CASH) in Trial Readiness Project. Part I: Event Rates, Functional and Patient Reported Outcomes. *Stroke*. 2023.
19. Polster SP, Cao Y, Carroll T, Flemming K, Girard R, Hanley D, Hobson N, Kim H, Koenig J, Koskimäki J, et al. Trial Readiness in Cavernous Angiomas With Symptomatic Hemorrhage (CASH). *Neurosurgery*. 2019;84:954–964. [PubMed: 29660039]
20. Kim H, Flemming KD, Nelson JA, Lui A, Majersik JJ, Cruz MD, Zabramski J, Trevizo O, Lanzino G, Zafar A, et al. Baseline Characteristics of Patients With Cavernous Angiomas With Symptomatic Hemorrhage in Multisite Trial Readiness Project. *Stroke*. 2021;52:3829–3838. [PubMed: 34525838]
21. Larsson HB, Courivaud F, Rostrup E, Hansen AE. Measurement of brain perfusion, blood volume, and blood-brain barrier permeability, using dynamic contrast-enhanced T(1)-weighted MRI at 3 tesla. *Magn Reson Med*. 2009;62:1270–1281. [PubMed: 19780145]
22. Polster SP, Stadnik A, Akers AL, Cao Y, Christoforidis GA, Fam MD, Flemming KD, Girard R, Hobson N, Koenig JI, et al. Atorvastatin Treatment of Cavernous Angiomas with Symptomatic Hemorrhage Exploratory Proof of Concept (AT CASH EPOC) Trial. *Neurosurgery*. 2019;85:843–853. [PubMed: 30476251]
23. Mabray MC, Caprihan A, Nelson J, McCulloch CE, Zafar A, Kim H, Hart BL, Morrison L. Effect of Simvastatin on Permeability in Cerebral Cavernous Malformation Type 1 Patients: Results from a Pilot Small Randomized Controlled Clinical Trial. *Transl Stroke Res*. 2020;11:319–321. [PubMed: 31643041]

24. Incerti I, Fusco M, Contarino VE, Siggillino S, Conte G, Lanfranconi S, Bertani GA, Gaudino C, d’Orio P, Pallini R, et al. Magnetic susceptibility as a 1-year predictor of outcome in familial cerebral cavernous malformations: a pilot study. *Eur Radiol.* 2023;33:4158–4166. [PubMed: 36602570]
25. Sone JY, Hobson N, Srinath A, Romanos SG, Li Y, Carrión-Penagos J, Shkoukani A, Stadnik A, Piedad K, Lightle R, et al. Perfusion and Permeability MRI Predicts Future Cavernous Angioma Hemorrhage and Growth. *J Magn Reson Imaging.* 2022;55:1440–1449. [PubMed: 34558140]
26. Sone JY, Li Y, Hobson N, Romanos SG, Srinath A, Lyne SB, Shkoukani A, Carrión-Penagos J, Stadnik A, Piedad K, et al. Perfusion and permeability as diagnostic biomarkers of cavernous angioma with symptomatic hemorrhage. *J Cereb Blood Flow Metab.* 2021;41:2944–2956. [PubMed: 34039038]
27. Liu T, Liu J, de Rochefort L, Spincemaille P, Khalidov I, Ledoux JR, Wang Y. Morphology enabled dipole inversion (MEDI) from a single-angle acquisition: comparison with COSMOS in human brain imaging. *Magn Reson Med.* 2011;66:777–783. [PubMed: 21465541]
28. Liu T, Khalidov I, de Rochefort L, Spincemaille P, Liu J, Tsiouris AJ, Wang Y. A novel background field removal method for MRI using projection onto dipole fields (PDF). *NMR Biomed.* 2011;24:1129–1136 [PubMed: 21387445]

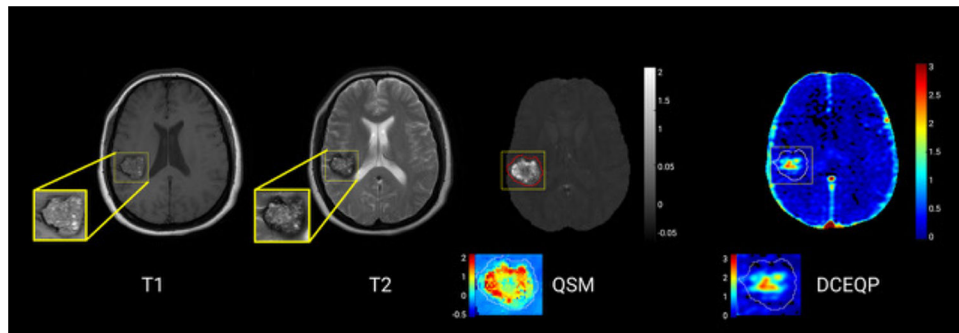
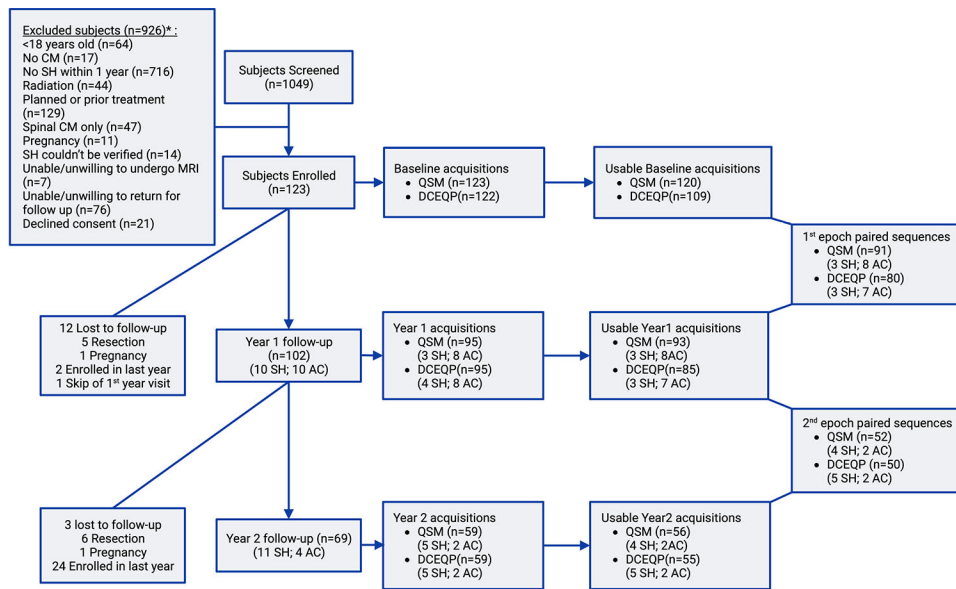


Figure 1. Illustration of conventional MRI axial images with (left to right) T1-weighted sequence, T2-weighted sequence, QSM, and DCEQP assessments of CM lesion with SH. The regions of interest for QSM and DCQEP assessments include the whole lesion as delineated on T2-weighted sequence. Note the maximal QSM values in the hemosiderin ring at the lesion periphery, while the maximal permeability values are within the core of the lesion.



*One subject could meet multiple exclusion criteria

Figure 2. Flow chart of screened, excluded and enrolled subjects with yearly follow-up and contribution to research imaging acquisitions, usability and QSM/DCEQP pairs analyzed.

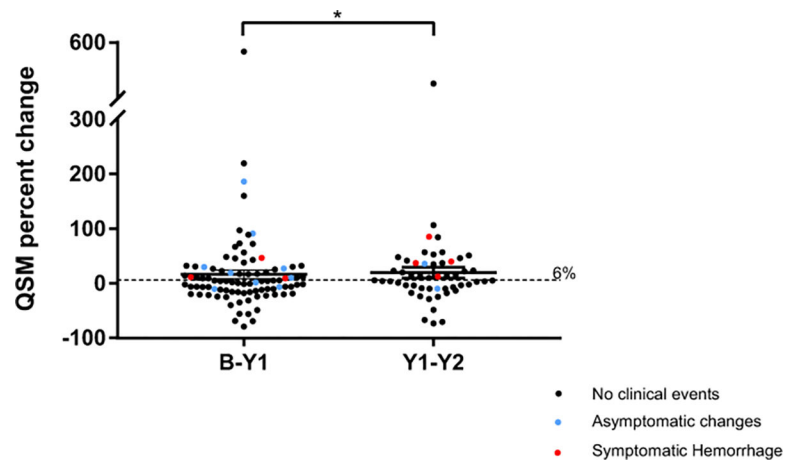


Figure 3.

QSM percent change during the 1st and 2nd follow-up years. QSM yearly-change during epoch 1 (mean +16.33; SD 74.93) was significantly lower ($p=0.033$) than in epoch 2 (mean +19.61; SD 70.96). Red dots represent SH; blue dots represent AC; and black dots represent no clinical event detected.

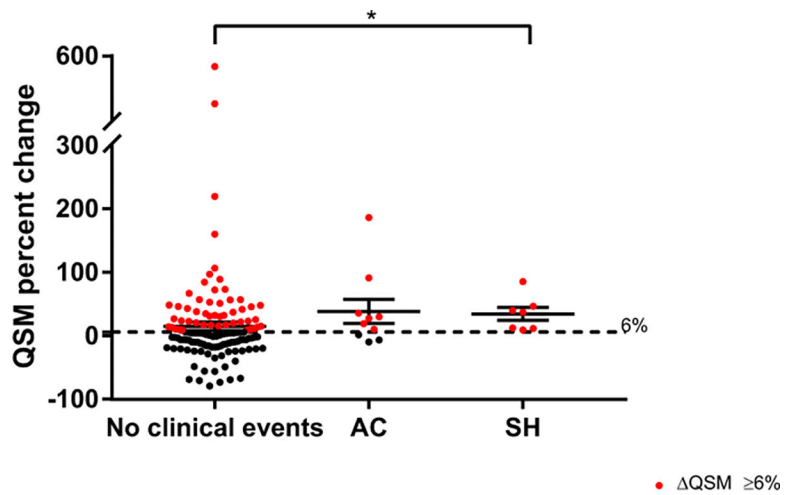


Figure 4.

QSM yearly percent change for cases with SH, AC and no clinical events detected during the same epoch as paired biomarker assessment. No significant differences in percent yearly-change in mean lesional QSM between cases with SH (mean +34.64; SD 27.17) and AC (mean +38.53; SD 59.36) during the same epoch. QSM changes with SH events were significantly higher than QSM change in cases with no clinical events (p 0.019). Red dots represent QSM pairs that meet the threshold biomarker $QSM \geq 6\%$.

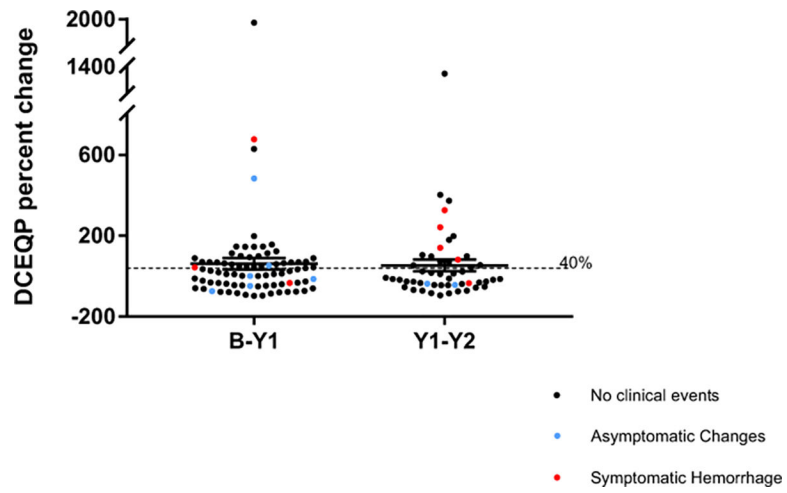


Figure 5. DCEQP percent change during the 1st and 2nd follow-up years. DCEQP yearly-change during the epoch 1 (mean +61.62; SD +248.8) was not significantly different from the change during epoch 2 (mean +52.45; SD +206.4). Red dots represent SH; blue dots represent AC; and black dots represent no clinical event detected.

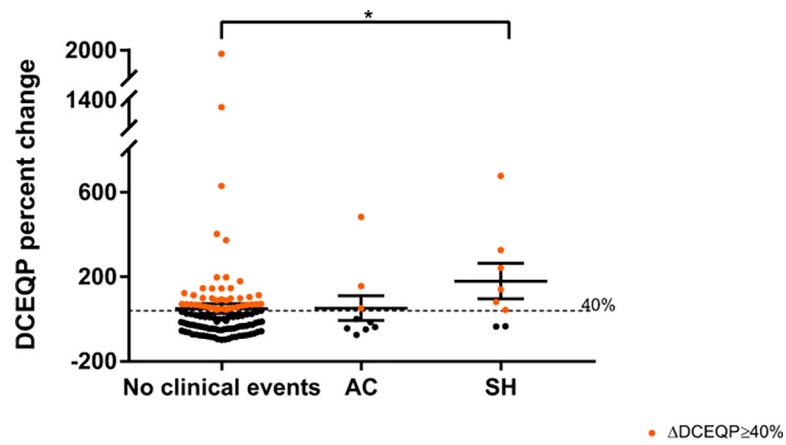


Figure 6.

DCEQP yearly percent change for SH, AC and no clinical events detected during the same epoch as paired biomarker assessment. There was significantly higher percent change in mean lesional DCEQOP (mean +179.9; SD +237.4) in cases with SH events than in those without detected clinical events (mean +49.92; SD +235.5) (p 0.030). No significant difference in yearly DCEQP change between AC events (mean +52.45; SD +175.8) and either SH events or cases with no clinical events. Orange dots represent DCEQP pairs that meet the threshold biomarker $\Delta\text{DCEQP} \geq 40\%$.